The 12th IEEE International Workshop on Advanced Motion Control
March 25-27, 2012, Sarajevo, Bosnia and Herzegovina

Analysis of Actuator Redundancy Resolution Methods for Bi-articularly Actuated Robot Arms

Valerio Salvucci
Department of Advanced Energy Engineering
The University of Tokyo
5-1-5 Kashiwanoha, Kashiwa, Chiba, Japan
Email:valerio@hori.k.u-tokyo.ac.jp

Sehoon Oh and Yoichi Hori
Department of Electrical Engineering
University of Tokyo, 3-7-1
Hongo Bunkyoku Tokyo, Japan
Email:sehoon@hori.k.u-tokyo.ac.jp, hori@k.u-tokyo.ac.jp

***Abstract*—Bi-articular actuators — actuators that span two joints — are rising interest in robot application because they increase stability, optimize force production, and reduce the non-linearity of the end effector force as a function of force direction. In this paper, we propose an approach to resolve actuator redundancy for bi-articularly actuated robot arms in which the three actuators produce maximum joint actuator torques that differs among each other. A closed form solution based on the infinity norm is derived. The proposed infinity norm based approach is compared with the conventional 1-norm and 2-norm based methods. Under the same actuator limitations, the maximum end effector force produced with the proposed method is significantly greater than the one produced by the conventional methods. The proposed closed form solution is suitable for redundant systems with three inputs and two outputs, bringing the advantage of an higher maximum output without the need for iterative algorithms.**

I. Introduction

Robot arms presenting animal musculo-skeletal characteristics such as bi-articular actuators — actuators that span two joints — have been proposed for more than two decades [1]. In recent years there has been increasing attention on such animal inspired robot arms, both in hardware and control design aspects.Regarding the hardware design, bi-articularly actuated robots have been realized by means of pneumatic actuators [2], [3], and motors with transmissions systems based on pulleys [4], [5], planetary gears , [6], [7], wires [8], [9], and passive springs [10], [11].

All these robots are driven by more actuators than joints, resulting therefore in actuator redundancy. In order to resolve the actuator redundancy problem due to the presence of bi-articular actuators, many approaches have been proposed.

In [12] several animal inspired approaches such as fatigue minimization, muscle force minimization, total muscle metabolic energy consumption, total muscle stress minimization are compared among each others. Among these approaches, the muscle force minimization [13] is implemented on robot applications using the $1-norm$.

Approaches based on pseudo-inverse matrices are used in the control design for kinematically redundant robot arm [14], [15]. Pseudo-inverse matrices are also used for actuator redundancy resolution [5], [16]. Moore-Penrose is the simplest pseudo-inverse matrix, and correspond to the minimization of the euclidean norm ($2-norm$) [17].

Iterative algorithms based on $\infty-norm$ optimization criteria have been used to resolve redundancy in kinematically redundant robot arms [18], [19]. In this paper the $\infty-norm$ norm is used to resolve the actuator redundancy for bi-articularly actuated robot arms. Differently from our previous work [20], the here proposed $\infty-norm$ based approach is extended also to the case in which the three actuators produce different maximum joint actuator torque among each other. A closed form solution based on a piecewise linear function for the infinity norm approach is proposed. The $\infty-norm$ approach allows to minimize the necessary maximum torque at each joint for a given force at end effector. Therefore it is an approach to optimize actuators design for robot arm equipped with by bi-articular actuators.

In addition, the proposed $\infty-norm$ is analytically compared with the traditional $1-norm$ and $2-norm$ approaches both in terms of joint actuator input torques and maximum output force at the end effector.

In Section II main features and statics of robot arms equipped with bi-articular actuators are described. Then, in Section III, three approaches for torque distribution resolution — minimization of muscle force ($1-norm$), $2-norm$ and $\infty-norm$ — are introduced. In Section IV the characteristics of $1-norm$, $2-norm$ and $\infty-norm$ approaches are analyzed in terms of joint actuator input torques and maximum output force at the end effector. Finally, in Section V, the advantages of the proposed optimization criteria are summarized.

II. Characteristics and Modeling of Robot Arm with Bi-articular Actuators

In conventional robot arms each joint is driven by one actuator. On the contrary, animal limbs present a complex musculoskeletal structure based on two types of muscles:

1) Monoarticular: the contraction of one of these muscles produces a torque on one joint.
2) Bi-articular: the contraction of one of these muscles produces the same torque on two consecutive joints at the same time. Gastrocnemius is an example of bi-articular muscle in the human leg.

A simplified model of the complex animal musculoskeletal system is shown in Fig. 1. This model is based on 6 contractile

978-1-4577-1073-5/12/$26.00 ©2012 IEEE

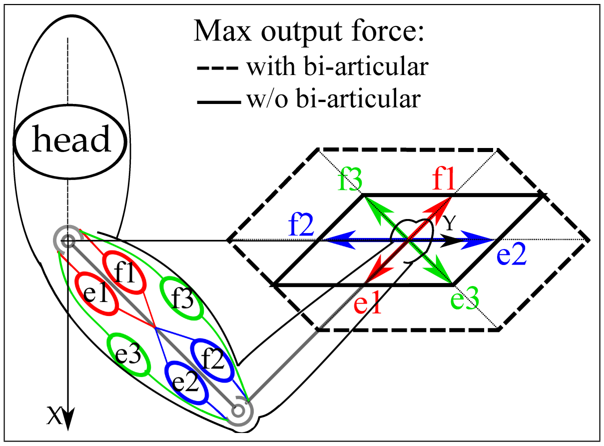

Fig. 1. Two-link arm with four mono- and two bi-articular muslces: model and resulting forces at the end effector

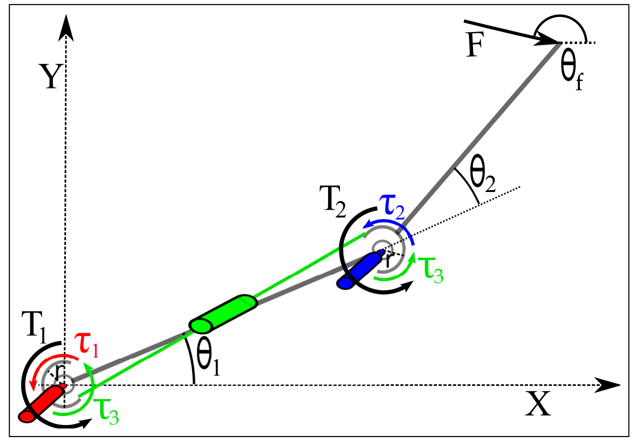

Fig. 2. Statics of two-link arm with four mono- and two bi-articular actuators

actuators — extensors (e1, e2 and e3) and flexors (f1, f2 and f3) — coupled in three antagonistic pairs:

- e1–f1 and e2–f2: couples of mono-articular actuators that produce torques about joint 1 and 2, respectively.
- e3–f3: couple of bi-articular actuators that produce torque about joint 1 and 2 contemporaneously.

Robot arms driven by bi-articular actuators have numerous advantages: dramatical increase in range of end effector impedance which can be achieved without feedback [1], realization of path tracking and disturbance rejection using just feedforward control [21], improvement of balance control for jumping robots that do not use force sensors [22]. Moreover, multi-joints actuators such as tri-articular actuators, increase the efficiency in the output force for robot arm [4]. Another advantage of robot arm equipped with bi-articular actuators is the ability to produce a more homogeneously distributed maximum output force at the end effector [20], [23].

III. Actuator Redundancy Problem and Resolution Methods

The resulting statics of the bi-articularly actuated arm of Fig. 1 are shown in Fig. 2, where:

$$T_1 = \tau_1 + \tau_3 \tag{1}$$
$$T_2 = \tau_2 + \tau_3 \tag{2}$$

- The total torques about joint 1 and 2 are T_1 and T_2, respectively.
- The torques produced by mono-articular actuators about joints 1 and 2 are τ_1 and τ_2, respectively. They are calculated from the actuator input forces e_i and f_i for $i = (1, 2)$ as:
$$\tau_1 = (f_1 - e_1)r \tag{3}$$
$$\tau_2 = (f_2 - e_2)r \tag{4}$$
where r is the distance between the joint axis and the point where the muscle force is applied, consider to be the same for all the muscles and all joint angles.
- The bi-articular torque produced about both joints is τ_3:
$$\tau_3 = (f_3 - e_3)r \tag{5}$$
- $\boldsymbol{F}$ is a general force at the end effector with magnitude F and direction θ_f.

A two-link robot arm with the statics shown in Fig. 2 presents actuator redundancy. Given τ_1, τ_2, and τ_3, it is possible to determine $\boldsymbol{T}$, and therefore $\boldsymbol{F}$ by using the Jacobian:

$$\begin{bmatrix} T_1 \\ T_2 \end{bmatrix} = J^T \begin{bmatrix} F_x \\ F_y \end{bmatrix} \tag{6}$$

where

$$J = \begin{bmatrix} -l_1\sin(\theta_1) - l_2\sin(\theta_1+\theta_2) & -l_2\sin(\theta_1+\theta_2) \\ l_1\cos(\theta_1) + l_2\cos(\theta_1+\theta_2) & l_2\cos(\theta_1+\theta_2) \end{bmatrix} \tag{7}$$

and F_x and F_y are the orthogonal projection of $\boldsymbol{F}$ on the x-axis and y-axis, respectively.

On the other hand, given $\boldsymbol{F}$, and therefore $\boldsymbol{T}$, it is generally not possible to determine uniquely τ_1, τ_2, and τ_3 (see (1) and (2)) due to the actuator redundancy. The problem represented by (1) and (2) is referred in the following as the redundancy actuator problem.

A. $1-norm$ approach

The actuator redundancy is resolved using the $1-norm$ by solving the following problem:

$$\begin{aligned} \min \quad & \left(\frac{|\tau_1|}{\tau_1^m} + \frac{|\tau_2|}{\tau_2^m} + \frac{|\tau_3|}{\tau_3^m}\right) \\ \text{s.t.} \quad & T_1 = \tau_1 + \tau_3 \\ & T_2 = \tau_2 + \tau_3 \end{aligned} \tag{8}$$

where $\tau_i^m, i = (1, 2, 3)$ is the maximum joint actuator torque that the actuator i can produce. The problem is solved using an iterative algorithm. Software tools as MATLAB can solve such problems.

B. 2-norm based approach

The actuator redundancy is resolved using the $2-norm$ by solving the following problem:

$$
\begin{aligned}
\min \quad & \sqrt{\frac{(\tau_1)^2}{(\tau_1^m)^2}+\frac{(\tau_2)^2}{(\tau_2^m)^2}+\frac{(\tau_3)^2}{(\tau_3^m)^2}} \\
\text{s.t.} \quad & T_1=\tau_1+\tau_3 \\
& T_2=\tau_2+\tau_3
\end{aligned} \tag{9}
$$

The solution of the problem expressed by (9) is:

$$\tau_1 = \frac{(T_1-T_2)(\tau_1^m)^2(\tau_3^m)^2+T_1(\tau_1^m)^2(\tau_2^m)^2}{(\tau_1^m)^2(\tau_2^m)^2+(\tau_1^m)^2(\tau_3^m)^2+(\tau_2^m)^2(\tau_3^m)^2} \tag{10}$$

$$\tau_2 = \frac{T_2(\tau_1^m)^2(\tau_2^m)^2+(T_2-T_1)(\tau_2^m)^2(\tau_3^m)^2}{(\tau_1^m)^2(\tau_2^m)^2+(\tau_1^m)^2(\tau_3^m)^2+(\tau_2^m)^2(\tau_3^m)^2} \tag{11}$$

$$\tau_3 = \frac{T_1(\tau_2^m)^2(\tau_3^m)^2+T_2(\tau_1^m)^2(\tau_3^m)^2}{(\tau_1^m)^2(\tau_2^m)^2+(\tau_1^m)^2(\tau_3^m)^2+(\tau_2^m)^2(\tau_3^m)^2} \tag{12}$$

Proof of (10), (11), and (12) is reported in Appendix A.

If $\tau_1^m=\tau_2^m=\tau_3^m$ the solution becomes [20]:

$$\tau_1 = \frac{2}{3}T_1-\frac{1}{3}T_2 \tag{13}$$

$$\tau_2 = -\frac{1}{3}T_1+\frac{2}{3}T_2 \tag{14}$$

$$\tau_3 = \frac{1}{3}T_1+\frac{1}{3}T_2 \tag{15}$$

C. Infinity norm based approach

The actuator redundancy is resolved using the $\infty-norm$ by solving the following problem:

$$
\begin{aligned}
\min \quad & \max\left(\frac{|\tau_1|}{\tau_1^m},\frac{|\tau_2|}{\tau_2^m},\frac{|\tau_3|}{\tau_3^m}\right) \\
\text{s.t.} \quad & T_1=\tau_1+\tau_3 \\
& T_2=\tau_2+\tau_3
\end{aligned} \tag{16}
$$

The fact that three torque values are scaled by the respective maximum torque guarantees that the solution, when exists, does not violate any of the three constraints:

$$-\tau_1^m \le \tau_1 \le \tau_1^m \tag{17}$$

$$-\tau_2^m \le \tau_2 \le \tau_2^m \tag{18}$$

$$-\tau_3^m \le \tau_3 \le \tau_3^m \tag{19}$$

Let us define:

$$c_1 = \frac{\tau_3^m-\tau_1^m}{\tau_3^m+\tau_2^m} \tag{20}$$

$$c_2 = \frac{\tau_3^m+\tau_2^m}{\tau_3^m+\tau_1^m} \tag{21}$$

$$c_3 = \frac{\tau_3^m-\tau_2^m}{\tau_3^m+\tau_1^m} \tag{22}$$

The three parameters c_1, c_2, and c_3 are defined for any maximum joint actuator torque, and are constant. A closed form solution of the problem (16) is determined on the basis of the values of T_1 and T_2 as follows:

$$\tau_1 = \begin{cases} (T_1-T_2)\frac{\tau_1^m}{\tau_1^m+\tau_2^m} & \text{if } case_1 \\ T_1-T_2\frac{\tau_3^m}{\tau_2^m+\tau_3^m} & \text{if } case_2 \\ T_1\frac{\tau_1^m}{\tau_1^m+\tau_3^m} & \text{if } case_3 \end{cases} \tag{23}$$

$$\tau_2 = \begin{cases} (T_2-T_1)\frac{\tau_2^m}{\tau_1^m+\tau_2^m} & \text{if } case_1 \\ T_2\frac{\tau_2^m}{\tau_2^m+\tau_3^m} & \text{if } case_2 \\ T_2-T_1\frac{\tau_3^m}{\tau_1^m+\tau_3^m} & \text{if } case_3 \end{cases} \tag{24}$$

$$\tau_3 = \begin{cases} \frac{T_1\tau_2^m+T_2\tau_1^m}{\tau_1^m+\tau_2^m} & \text{if } case_1 \\ T_2\frac{\tau_3^m}{\tau_2^m+\tau_3^m} & \text{if } case_2 \\ T_1\frac{\tau_3^m}{\tau_1^m+\tau_3^m} & \text{if } case_3 \end{cases} \tag{25}$$

where

$$
\begin{aligned}
case_1 = & (T_1 \le c_1T_2 \text{ and } T_2 \ge c_3T_1) \\
& \text{or } (T_1 > c_1T_2 \text{ and } T_2 < c_3T_1) \\
case_2 = & (T_1 \ge c_1T_2 \text{ and } T_2 \ge c_2T_1) \\
& \text{or } (T_1 < c_1T_2 \text{ and } T_2 < c_2T_1) \\
case_3 = & (T_2 \le c_2T_1 \text{ and } T_2 \ge c_3T_1) \\
& \text{or } (T_2 > c_2T_1 \text{ and } T_2 < c_3T_1)
\end{aligned}
$$

Proof of (23), (24), and (25) is reported in Appendix B.

It is trivial to verify that the three linear piecewise functions (23), (24), and (25) are continuous in all the domain $D=(T_1,T_2)$.

In summary, the values of τ_1, τ_2, and τ_3 that produce a given $\boldsymbol{F}$ at the end effector, are determined as follows:

1) Calculate the desired joint torques $\boldsymbol{T}=J^T\boldsymbol{F}$.
2) According to calculated T_1 and T_2, the three desired joint actuator torques are directly determined using the three piecewise linear function (23), (24), and (25).

When all the actuators produce the same maximum joint actuator torque, that is $\tau_1^m=\tau_2^m=\tau_3^m$, $c_1=c_3=0$ and $c_2=1$, and the solution becomes as in the following [20]:

$$\tau_1 = \begin{cases} \frac{T_1-T_2}{2} & \text{if } T_1T_2 \le 0 \\ T_1-\frac{T_2}{2} & \text{if } T_1T_2>0 \text{ and } |T_1| \le |T_2| \\ \frac{T_1}{2} & \text{if } T_1T_2>0 \text{ and } |T_1|>|T_2| \end{cases} \tag{26}$$

$$\tau_2 = \begin{cases} \frac{T_2-T_1}{2} & \text{if } T_1T_2 \le 0 \\ \frac{T_2}{2} & \text{if } T_1T_2>0 \text{ and } |T_1| \le |T_2| \\ T_2-\frac{T_1}{2} & \text{if } T_1T_2>0 \text{ and } |T_1|>|T_2| \end{cases} \tag{27}$$

$$\tau_3 = \begin{cases} \frac{T_1+T_2}{2} & \text{if } T_1T_2 \le 0 \\ \frac{T_2}{2} & \text{if } T_1T_2>0 \text{ and } |T_1| \le |T_2| \\ \frac{T_1}{2} & \text{if } T_1T_2>0 \text{ and } |T_1|>|T_2| \end{cases} \tag{28}$$

IV. RESULTS

In the following a two-links robot arm with $l_1=15$ m and $l_2=12$ m is taken into account. The maximum joint actuator torques are $\tau_1^m=16$ N, $\tau_2^m=14$ N, and $\tau_3^m=18$ N.

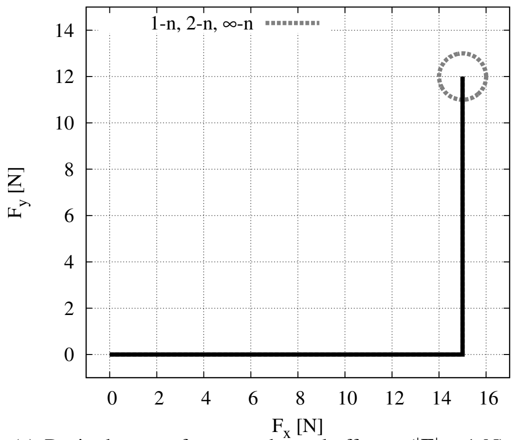

(a) Desired output force ate the end effector ($|\mathbf{F}| = 1$ N)

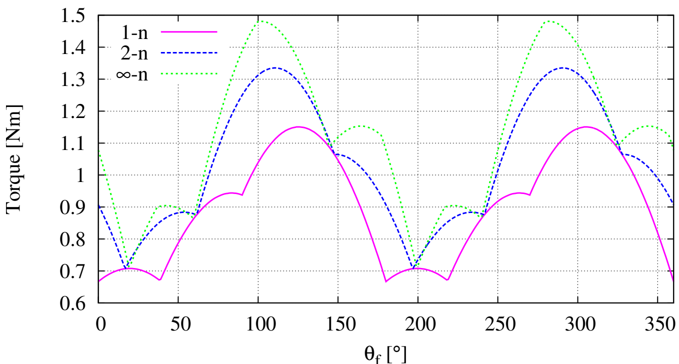

(b) $\frac{|\tau_1|}{\tau_1^m} + \frac{|\tau_2|}{\tau_2^m} + \frac{|\tau_3|}{\tau_3^m}$ for $1-norm$, $2-norm$ and $\infty-norm$ approaches

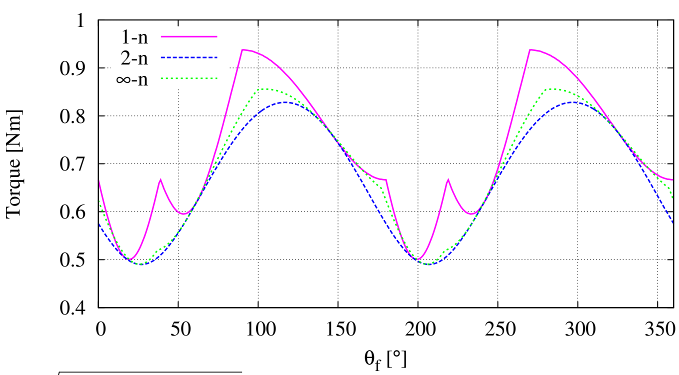

(c) $\sqrt{\frac{(\tau_1)^2}{(\tau_1^m)^2} + \frac{(\tau_2)^2}{(\tau_2^m)^2} + \frac{(\tau_3)^2}{(\tau_3^m)^2}}$ for $1-norm$, $2-norm$ and $\infty-norm$ approaches

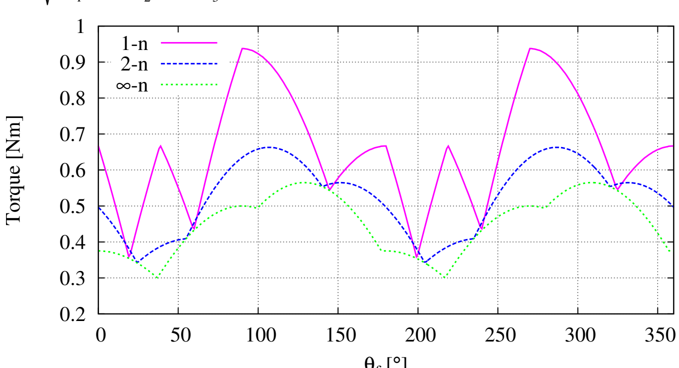

(d) $\max\left(\frac{|\tau_1|}{\tau_1^m}, \frac{|\tau_2|}{\tau_2^m}, \frac{|\tau_3|}{\tau_3^m}\right)$ for $1-norm$, $2-norm$ and $\infty-norm$ approaches

Fig. 3. Comparison of joint actuators torque inputs among $1-norm$, $2-norm$ and $\infty-norm$ approaches

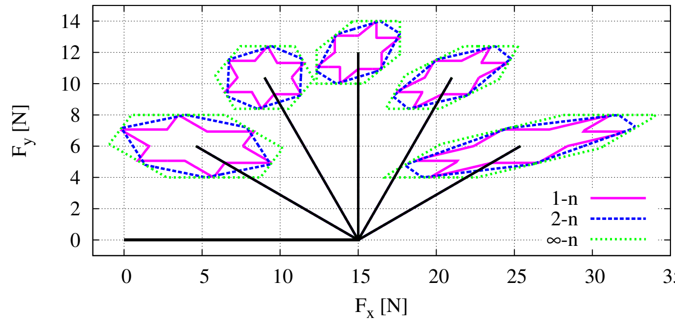

Fig. 4. Comparison of maximum output force at end effector — $\theta_2 = (30, 60, 90, 120, 150°)$

A. Joint actuator torques comparison

Fig. 3 shows a comparison of actuator joint torques input for three actuator redundancy resolution methods, $1-norm$, $2-norm$ and $\infty-norm$. The desired output is an output force $\mathbf{F}$ at the end effector with magnitude 1 N in all the directions for $\theta_2 = 90°$. The compared values are $\frac{|\tau_1|}{\tau_1^m} + \frac{|\tau_2|}{\tau_2^m} + \frac{|\tau_3|}{\tau_3^m}$ (Fig. 3(b)), $\sqrt{\frac{(\tau_1)^2}{(\tau_1^m)^2} + \frac{(\tau_2)^2}{(\tau_2^m)^2} + \frac{(\tau_3)^2}{(\tau_3^m)^2}}$ (Fig. 3(c)), and $\max\left(\frac{|\tau_1|}{\tau_1^m}, \frac{|\tau_2|}{\tau_2^m}, \frac{|\tau_3|}{\tau_3^m}\right)$ (Fig. 3(d)).

The advantage of $1-norm$ approach is that requires the lowest sum of actuator joint torques (Fig. 3(b)). The advantage of $\infty-norm$ is that allows to minimize the maximum actuator joint torques (Fig. 3(d)). $2-norm$ is in between the other two approaches. The same results can be obtained for $\theta_2 \neq 90°$.

B. Maximum output force

Fig. 4 shows the maximum output force at end effector for $\theta_2 = (30, 60, 90, 120, 150°)$. Given the same maximum actuator joint torques $\infty-norm$ can produce the greatest force at end effector. This is the great advantage of the $\infty-norm$ approach. $1-norm$ produces the lower output force, while $2-norm$ is in between the other two approaches.

V. Conclusions

In this paper, we propose an approach to resolve actuator redundancy for bi-articularly actuated robot arms in which the three actuators produce maximum joint actuator torques that differs among each other. Moreover, the proposed $\infty-norm$ based approach is compared with the muscle force minimization approach ($1-norm$) and with the Moore-Penrose pseudoinverse matrix ($2-norm$) approaches. Main results are:

- The proposed $\infty-norm$ approach allows the maximization of output force at the end effector.
- The $1-norm$ approach minimizes the total muscle force input, but the maximum force space is the smallest. If a circular output force the end effector is desired, this approach requires the highest joint actuator torque.
- The $2-norm$ approach is in between $1-norm$ and $\infty-norm$ in terms of both maximum force space and total torque input.

ACKNOWLEDGMENT

This work is supported by Inamori Foundation

APPENDIX A
PROOF OF CLOSED FORM SOLUTION FOR THE 2-NORM APPROACH

The problem expressed by (9) is written for a simpler notation as:

$$\begin{array}{ll} \min & \sqrt{\frac{(x)^2}{(mx)^2}+\frac{(y)^2}{(my)^2}+\frac{(z)^2}{(mz)^2}} \\ \text{s.t.} & T_1 = x+z \\ & T_2 = y+z \end{array} \tag{29}$$

where T_1 and T_2 are the desired joint torques (known), x, y, and z are the desired joint actuator torques τ_1, τ_2, and τ_3 (unknown), respectively; $mx = \tau_1^m$, $my = \tau_2^m$, and $mz = \tau_3^m$. Taking into account $\mathbb{R}^3$, the solution (x, y, z) which satisfy $\sqrt{\frac{(x)^2}{(mx)^2}+\frac{(y)^2}{(my)^2}+\frac{(z)^2}{(mz)^2}}$ has to meet the following three requirements:

1) To be on the line defined by

$$T_1 = x+z \tag{30}$$
$$T_2 = y+z \tag{31}$$

2) To be on the ellipsoid surface defined by:

$$\frac{x^2}{mx^2}+\frac{y^2}{my^2}+\frac{z^2}{mz^2} = k \tag{32}$$

where k is a constant.

3) The plane passing through the line defined by (30) and (31) has to be tangent to the ellipsoid defined by (32). Hence:

$$\frac{1}{mx^2}\frac{\partial x^2}{\partial x}+\frac{1}{my^2}\frac{\partial y^2}{\partial y}+\frac{1}{mz^2}\frac{\partial z^2}{\partial z} = 0 \tag{33}$$

Combining (30), (31), (32), (33) straightforward follows the solution of the problem (29):

$$x = \frac{(T_1-T_2)mx^2mz^2+T_1mx^2my^2}{mx^2my^2+mx^2mz^2+my^2mz^2} \tag{34}$$

$$y = \frac{T_2mx^2my^2+(T_2-T_1)my^2mz^2}{mx^2my^2+mx^2mz^2+my^2mz^2} \tag{35}$$

$$z = \frac{T_1my^2mz^2+T_2mx^2mz^2}{mx^2my^2+mx^2mz^2+my^2mz^2} \tag{36}$$

Equations (34), (35), and (36) correspond to (10), (11), and (12), respectively.

APPENDIX B
PROOF OF CLOSED FORM SOLUTION FOR THE INFINITY-NORM APPROACH

The problem expressed by (16) is written for a simpler notation as:

$$\begin{array}{ll} \min & \max\left(\frac{|x|}{mx}, \frac{|y|}{my}, \frac{|z|}{mz}\right) \\ \text{s.t.} & T_1 = x+z \\ & T_2 = y+z \end{array} \tag{37}$$

where T_1 and T_2 are the desired joint torques (known), x, y, and z are the desired joint actuator torques τ_1, τ_2, and τ_3 (unknown), respectively; $mx = \tau_1^m$, $my = \tau_2^m$, and $mz = \tau_3^m$.

A closed form solution of (37) is determined in the following. The searched solution has to satisfy at least one of the three equations $\frac{|x|}{mx} = \frac{|y|}{my}$, $\frac{|y|}{my} = \frac{|z|}{mz}$, $\frac{|x|}{mx} = \frac{|z|}{mz}$. In fact, when one of three variable's absolute value decreases at least one of the other two increases. Therefore for any solution of the system with $\frac{|x|}{mx} \neq \frac{|y|}{my} \neq \frac{|z|}{mz}$ it is possible to decrease the higher value among the three so to be equal to at least one of the other two. Therefore the searched solution is one among the following six:

1) $\frac{x}{mx} = -\frac{y}{my}$

$$\left\{\begin{array}{l} x+z = T_1 \\ y+z = T_2 \\ \frac{x}{mx} = -\frac{y}{my} \end{array}\right. \Rightarrow \left\{\begin{array}{l} x = (T_1-T_2)\frac{mx}{my+mx} \\ y = (T_2-T_1)\frac{my}{my+mx} \\ z = T_2-(T_2-T_1)\frac{my}{my+mx} \end{array}\right. \tag{38}$$

2) $\frac{y}{my} = \frac{z}{mz}$

$$\left\{\begin{array}{l} x+z = T_1 \\ y+z = T_2 \\ \frac{y}{my} = \frac{z}{mz} \end{array}\right. \Rightarrow \left\{\begin{array}{l} x = T_1-T_2\frac{mz}{my+mz} \\ y = T_2\frac{my}{my+mz} \\ z = T_2\frac{mz}{my+mz} \end{array}\right. \tag{39}$$

3) $\frac{x}{mx} = \frac{z}{mz}$

$$\left\{\begin{array}{l} x+z = T_1 \\ y+z = T_2 \\ \frac{x}{mx} = \frac{z}{mz} \end{array}\right. \Rightarrow \left\{\begin{array}{l} x = T_1\frac{mx}{mz+mx} \\ y = T_2-T_1\frac{mz}{mz+mx} \\ z = T_1\frac{mz}{mz+mx} \end{array}\right. \tag{40}$$

4) $\frac{x}{mx} = \frac{y}{my}$

$$\left\{\begin{array}{l} x+z = T_1 \\ y+z = T_2 \\ \frac{x}{mx} = \frac{y}{my} \end{array}\right. \Rightarrow \left\{\begin{array}{l} x = (T_2-T_1)\frac{mx}{my-mx} \\ y = (T_2-T_1)\frac{my}{my-mx} \\ z = T_2-(T_2-T_1)\frac{my}{my-mx} \end{array}\right. \tag{41}$$

5) $\frac{y}{my} = -\frac{z}{mz}$

$$\left\{\begin{array}{l} x+z = T_1 \\ y+z = T_2 \\ \frac{y}{my} = -\frac{z}{mz} \end{array}\right. \Rightarrow \left\{\begin{array}{l} x = T_1-T_2\frac{mz}{mz-my} \\ y = -T_2\frac{my}{mz-my} \\ z = T_2\frac{mz}{mz-my} \end{array}\right. \tag{42}$$

6) $\frac{x}{mx} = -\frac{z}{mz}$

$$\left\{\begin{array}{l} x+z = T_1 \\ y+z = T_2 \\ \frac{x}{mx} = -\frac{z}{mz} \end{array}\right. \Rightarrow \left\{\begin{array}{l} x = -T_1\frac{mx}{mz-mx} \\ y = T_2-T_1\frac{mz}{mz-mx} \\ z = T_1\frac{mz}{mz-mx} \end{array}\right. \tag{43}$$

Let us define:

$$c_1 = \frac{mz-mx}{mz+my} \tag{44}$$

$$c_2 = \frac{mz+my}{mz+mx} \tag{45}$$

$$c_3 = \frac{mz-my}{mz+mx} \tag{46}$$

These values depend only on the hardware characteristics of the arm, therefore are constant. Among the six possible solutions the searched one is directly selected on the basis of T_1 and T_2 as follows (the variable subscript represents the respective equation number):

- If ($T_1 \le c_1 T_1$ and $T_2 \ge c_3 T_1$) or ($T_1 > c_1 T_2$ and $T_2 < c_3 T_1$):

$$\left|\frac{x_{(38)}}{mx}\right| = \left|\frac{y_{(38)}}{my}\right| \ge \left|\frac{z_{(38)}}{mz}\right| \tag{47}$$
$$|x_{(38)}| \le |x_{(39)}| \tag{48}$$
$$|y_{(38)}| \le |y_{(40)}| \tag{49}$$
$$|x_{(38)}| \le |x_{(41)}| \tag{50}$$
$$|x_{(38)}| \le |x_{(42)}|, \text{ if } mz \ge my \tag{51}$$
$$|y_{(38)}| \le |y_{(42)}|, \text{ if } mz < my \tag{52}$$
$$|x_{(38)}| \le |x_{(43)}|, \text{ if } mx \ge mz \tag{53}$$
$$|y_{(38)}| \le |y_{(43)}|, \text{ if } mx < mz \tag{54}$$

Therefore solution is (38). In this case, τ_1 in (23), τ_2 in (24), and τ_3 in (25), are equal to x in (38), y in (38), and z in (38), respectively.

- If ($T_1 \ge c_1 T_2$ and $T_2 \ge c_2 T_1$) or ($T_1 < c_1 T_2$ and $T_2 < c_2 T_1$):

$$\left|\frac{y_{(39)}}{my}\right| = \left|\frac{z_{(39)}}{mz}\right| \ge \left|\frac{x_{(39)}}{mx}\right| \tag{55}$$
$$|z_{(39)}| \le |z_{(38)}| \tag{56}$$
$$|y_{(39)}| \le |y_{(40)}| \tag{57}$$
$$|y_{(39)}| \le |y_{(41)}|, \text{ if } my \ge mx \tag{58}$$
$$|z_{(39)}| \le |z_{(41)}|, \text{ if } my < mx \tag{59}$$
$$|y_{(39)}| \le |y_{(42)}| \tag{60}$$
$$|y_{(39)}| \le |y_{(43)}|, \text{ if } mx \ge mz \tag{61}$$
$$|z_{(39)}| \le |z_{(43)}|, \text{ if } mx < mz \tag{62}$$

Therefore solution is (39). In this case, τ_1 in (23), τ_2 in (24), and τ_3 in (25), are equal to x in (39), y in (39), and z in (39), respectively.

- If ($T_2 \le c_2 T_1$ and $T_2 \ge c_3 T_1$) or ($T_2 > c_2 T_1$ and $T_2 < c_3 T_1$):

$$\left|\frac{x_{(40)}}{mx}\right| = \left|\frac{z_{(40)}}{mz}\right| \ge \left|\frac{y_{(40)}}{my}\right| \tag{63}$$
$$|z_{(40)}| \le |z_{(38)}| \tag{64}$$
$$|x_{(40)}| \le |x_{(39)}| \tag{65}$$
$$|x_{(40)}| \le |x_{(41)}|, \text{ if } mx \ge my \tag{66}$$
$$|z_{(40)}| \le |z_{(41)}|, \text{ if } mx < my \tag{67}$$
$$|x_{(40)}| \le |x_{(42)}|, \text{ if } my \ge mz \tag{68}$$
$$|z_{(40)}| \le |z_{(42)}|, \text{ if } my < mz \tag{69}$$
$$|x_{(40)}| \le |x_{(43)}| \tag{70}$$

Therefore solution is (40). In this case, τ_1 in (23), τ_2 in (24), and τ_3 in (25), are equal to x in (40), y in (40), and z in (40), respectively.

References

[1] N. Hogan, "Impedance control: An approach to manipulation: Part III—Applications," *Journal of Dynamic Systems, Measurement, and Control*, vol. 107, no. 1, pp. 17–24, Mar. 1985.

[2] R. Niiyama, S. Nishikawa, and Y. Kuniyoshi, "Athlete robot with applied human muscle activation patterns for bipedal running," in *Humanoid Robots (Humanoids), 2010 10th IEEE-RAS International Conference on*, 2010, pp. 498–503.

[3] K. Hosoda, Y. Sakaguchi, H. Takayama, and T. Takuma, "Pneumatic-driven jumping robot with anthropomorphic muscular skeleton structure," *Autonomous Robots*, vol. 28, no. 3, pp. 307–316, Dec. 2009.

[4] T. Tsuji, "A model of antagonistic triarticular muscle mechanism for lancelet robot," in *2010 11th IEEE International Workshop on Advanced Motion Control*. IEEE, Mar. 2010, pp. 496–501.

[5] K. Yoshida, N. Hata, S. Oh, and Y. Hori, "Extended manipulability measure and application for robot arm equipped with bi-articular driving mechanism," in *Industrial Electronics, 2009. IECON '09. 35th Annual Conference of IEEE*, 2009, pp. 3083–3088.

[6] Y. Kimura, S. Oh, and Y. Hori, "Novel robot arm with bi-articular driving system using a planetary gear system and disturbance observer," in *Advanced Motion Control, 2010 11th IEEE International Workshop on*, 2010, pp. 296–301.

[7] M. Shinohara, A. Umemura, T. Haneyoshi, and Y. Saito, "Coordination control of bi-articular robotic arm by motor drive with planetary gear," in *Power Electronics Conference (IPEC), 2010 International*, 2010, pp. 2551–2556.

[8] V. Salvucci, Y. Kimura, S. Oh, and Y. Hori, "BiWi: bi-articularly actuated and wire driven robot arm," in *IEEE International Conference on Mechatronics (ICM)*, Apr. 2011, pp. 827–832.

[9] M. A. Lewis and T. J. Klein, "Achilles: A robot with realistic legs," in *IEEE Biomedical Circuits and Systems Conference (BIOCAS)*, 2008.

[10] F. Iida, J. Rummel, and A. Seyfarth, "Bipedal walking and running with spring-like biarticular muscles," *Journal of Biomechanics*, vol. 41, no. 3, pp. 656–667, 2008.

[11] A. Seyfarth, F. Iida, R. Tausch, M. Stelzer, O. von Stryk, and A. Karguth, "Towards bipedal jogging as a natural result of optimizing walking speed for passively compliant Three-Segmented legs," *The International Journal of Robotics Research*, vol. 28, no. 2, pp. 257 –265, Feb. 2009.

[12] B. M. van Bolhuis and C. C. A. M. Gielen, "A comparison of models explaining muscle activation patterns for isometric contractions," *Biological Cybernetics*, vol. 81, no. 3, pp. 249–261, 1999.

[13] B. Yeo, "Investigations concerning the principle of minimal total muscular force," *Journal of Biomechanics*, vol. 9, no. 6, pp. 413–416, 1976.

[14] R. Patel, H. Talebi, J. Jayender, and F. Shadpey, "A robust position and force control strategy for 7-DOF redundant manipulators," *Mechatronics, IEEE/ASME Transactions on*, vol. 14, no. 5, pp. 575–589, 2009.

[15] G. White, R. Bhatt, C. Tang, and V. Krovi, "Experimental evaluation of dynamic redundancy resolution in a nonholonomic wheeled mobile manipulator," *Mechatronics, IEEE/ASME Transactions on*, vol. 14, no. 3, pp. 349–357, 2009.

[16] A. Z. Shukor and Y. Fujimoto, "Modelling and control of redundant robot manipulator using spiral motor," in *6th Europe-Asia Congress on Mechatronics EAM, Proceedings of*, 2010, pp. 59–65.

[17] C. A. Klein and C. H. Huang, "Review of pseudoinverse control for use with kinematically redundant manipulators," *IEEE Transactions on Systems, Man, and Cybernetics*, vol. 13, pp. 245–250, 1983.

[18] I. Shim and Y. Yoon, "Stabilized minimum Infinity-Norm torque solution for redundant manipulators," *Robotica*, vol. 16, no. 02, pp. 193–205, 1998.

[19] X. Zhu, G. Tao, B. Yao, and J. Cao, "Adaptive robust posture control of parallel manipulator driven by pneumatic muscles with redundancy," *Mechatronics, IEEE/ASME Transactions on*, vol. 13, no. 4, pp. 441–450, 2008.

[20] V. Salvucci, Y. Kimura, S. Oh, and Y. Hori, "Experimental verification of infinity norm approach for force maximization of manipulators driven by bi-articular actuators," in *American Control Conference (ACC)*, 2011.

[21] K. Yoshida, T. Uchida, and Y. Hori, "Novel FF control algorithm of robot arm based on bi-articular muscle principle - emulation of muscular viscoelasticity for disturbance suppression and path tracking," in *Industrial Electronics Society, 2007. IECON 2007. 33rd Annual Conference of the IEEE*, 2007, pp. 310–315.

[22] S. Oh, Y. Kimura, and Y. Hori, "Reaction force control of robot manipulator based on biarticular muscle viscoelasticity control," in *Advanced Intelligent Mechatronics (AIM), 2010 IEEE/ASME International Conference on*, 2010, pp. 1105–1110.

[23] T. Fujikawa, T. Oshima, M. Kumamoto, and N. Yokoi, "Output force at the endpoint in human upper extremities and coordinating activities of each antagonistic pairs of muscles." *Transactions of the Japan Society of Mechanical Engineers. C*, vol. 65, no. 632, pp. 1557–1564, 1999.